Photovoltaic effect in semiconductor nanocrystals embedded into amorphous silicon *p-n* junction

Sergei G. Krivoshlykov[a] and Valery I. Rupasov[b]
ANTEOS, Inc., Shrewsbury, MA 01545, USA

(Received 15 February 2008; accepted 24 June 2008; published online 30 July 2008)

We report experimental demonstration of photovoltaic effect in nanocomposite amorphous silicon *p-i-n* junction comprising a thin film of lead selenide (PbSe) nanocrystals deposited on a *p*-type crystalline silicon wafer and overcoated with *n*-type layer of hydrogenated amorphous silicon.
 [DOI: 10.1063/1.2958235]

The recently discovered carrier multiplication (CM) effect[1–4] resulting in ultraefficient generation of two (or several) electron-hole pairs (excitons) in colloidal semiconductor nanocrystals (NCs) by single absorbed photons opens the door to dramatic enhancement of the energy conversion efficiency of thin film photovoltaic materials and solar cells. However, the characteristic time of Auger recombination of biexcitons in NCs is measured to be on the order of 200–300 ps.[5] Therefore, for practical implementations of high-efficiency NC solar cells taking advantage of the CM effect, one needs to solve the problem of fast and efficient ejection of photogenerated electrons and holes from NCs and their further spatial separation for times shorter than the Auger recombination time. This problem can be solved by placing a NC material in a strong built-in electrical field of the *p-i-n* junction, in which the intrinsic layer made of NC material is sandwiched between *p*- and *n*-type semiconductor layers.[6]

The nanocomposite *p-i-n* junction using CdSe NC layer and GaN *p*- and *n*-type layers have been already fabricated and its operation as an efficient light-emitting diode has been demonstrated.[7] To avoid high-temperature degradation of NC layer, the authors developed a special method for low-temperature deposition ($T<400$ °C) of GaN layer on the NC material.

Another possible design employing amorphous silicon material[8] has been recently proposed in our patent application.[9] Here we report experimental demonstration of the photovoltaic effect in PbSe NC layer deposited on *p*-type crystalline silicon (*c*-Si) wafer and covered by *n*-type hydrogenated amorphous silicon (*a*-Si) layer. Low-temperature deposition of *a*-Si ($T=160$ °C) prevents any possible high-temperature degradation of physical properties of NCs.

Figure 1 shows energy band diagrams of *n*-type *a*-Si, PbSe NCs, and *p*-type *c*-Si. Dotted lines show positions of the Fermi energies of *a*-Si and *c*-Si. The inset in Fig. 1 shows schematic of our model device designed to study the main features of the nanocomposite photovoltaic structures. The energy band alignment of *c*-Si and *a*-Si ensures the effective energy gap of *p-i-n* junction on the order of 1.1–1.2 eV matching the position and size of the effective energy gap of PbSe NCs ($E_g^*=0.8$ eV).

We used a heavily doped *p*-type *c*-Si wafer having thickness of 250–300 μm and resistivity in the range of 0.001–0.005 Ω cm. At such a resistivity, the density of acceptors in bulk silicon ranges in the interval 2.07×10^{19}–1.16×10^{20} cm^{-3}, and the Fermi energy is located slightly below the valence band edge. The thickness of depletion layer in *c*-Si is negligibly small (less than 1 nm). Therefore, we can ignore any possible contribution of *c*-Si into photocurrent. At density of donors of approximately 2×10^{16} cm^{-3} used in the fabrication of *n*-type *a*-Si, shift of the Fermi energy in *a*-Si is estimated to be about 0.4 eV. Thickness of the depletion layer in *a*-Si is estimated to be of the order of 50 nm. Thus, the fabricated *a*-Si layer having thickness of 20–30 nm can contribute to photocurrent at the light frequencies exceeding effective bandgap of the material (1.8–1.9 eV). Note also that a relatively thin *a*-Si layer in our model device is practically fully depleted.

The design of model device is not quite optimal. There are potential barriers of 0.3 eV for transfer of electrons from NCs to the conduction band of *a*-Si, and of 0.17 eV for transfer of holes from NCs to the valence band of *c*-Si. From one side, the potential barriers are necessary to provide required confinement for charge carriers in NCs, but from the other side they may prevent charge ejection from NCs. However, strong built-in electric field of the *p-n* junction ($E\sim10^5$ eV/cm) ensures charge ejection through the potential barriers.

The NC film was fabricated using drop casting from a chloroform solution of PbSe nanocrystals having S–S absorption peak at 1526 nm. Thickness of the NC film is estimated to be on the order of 20–25 nm (i.e., 3–4 ML). For formation of the nanocrystal layer with sufficiently good

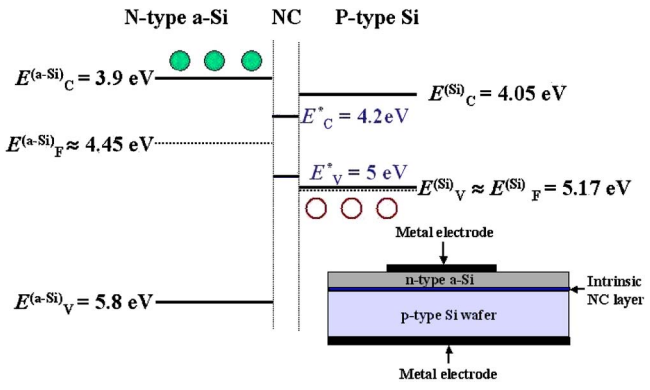

FIG. 1. (Color online) Energy band diagram for *n*-type *a*-Si, PbSe nanocrystals, and *p*-type *c*-Si. The dotted lines show positions of the Fermi energies of *a*-Si and *c*-Si. The inset shows the schematic of model device.

[a]Electronic mail: anteosinc@aol.com.
[b]Electronic mail: valery_rupasov@hotmail.com.

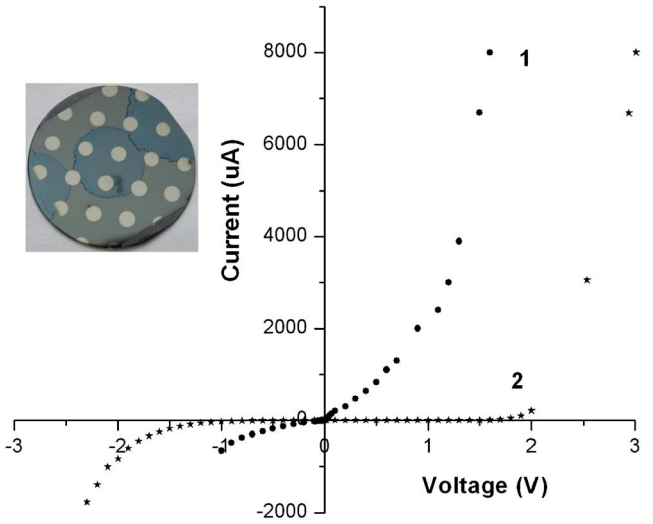

FIG. 2. (Color online) Current-voltage curve for pristine *a*-Si-*c*-Si *p-n* junction (1) and nanocomposite *p-i-n* junction with nanocrystal intrinsic layers (2). The inset shows the picture of the fabricated device.

conductivity we treated the NC in methanol[10–12] to partially remove oleic acid ligands, which are usually attached to surface of the NCs to prevent their precipitation in solution. Finally, the nanocrystals have been dissolved in hexane/octane solution, 4:1 by volume. Dropping such a solution on polished surface of *c*-Si wafer resulted in formation of a uniform nanocrystal film. Deposition of *n*-doped amorphous silicon on top of the fabricated NC film was performed using plasma-enhanced chemical-vapor deposition (PECVD) at concentration of doping gas of about 6%. By measuring absorption and luminescence spectra of NC film deposited on a reference glass substrate we verified that deposition of amorphous silicon did not cause any degradation of NCs. Finally, aluminum electrodes were sputtered on top of *n*-doped *a*-Si layer. Bottom contact was fabricated using conducting silver paste. An example of the fabricated device is shown in inset of Fig. 2.

Figure 2 shows current-voltage characteristic of the fabricated devices. At forward bias the current exhibits typical exponential dependence on the applied positive voltage. Curve 1 corresponds to pristine *p-n* junction. Thickness of *n*-type *a*-Si film is less than depth of depletion layer and much less than the diffusion length. This explains a deviation of the *I-V* curve at reverse bias form typical behavior of sufficiently thick *p-n* junction. Curve 2 illustrates a dramatic change in the current-voltage characteristic after introducing the intrinsic layer of nanocrystals. It can be explained by much smaller conductivity of the NC material.

Figure 3(a) shows short circuit photocurrent in the fabricated model devices normalized to the power of the incident laser beam at various wavelengths. The group of curves 1 represents photoresponse of various identical samples of pristine silicon *p-n* junctions. Increasing the photoresponse with wavelength reflects wavelength dependence of light absorption in silicon, which is strongest in the ultraviolet region at 325 nm. Points 2 marked in Fig. 3 with stars represent photoresponse of the device employing the NCs with partially removed ligands as an intrinsic layer. In spite of the fact that resistance of the NC device exceeds that of silicon device almost by four orders of magnitude, both devices

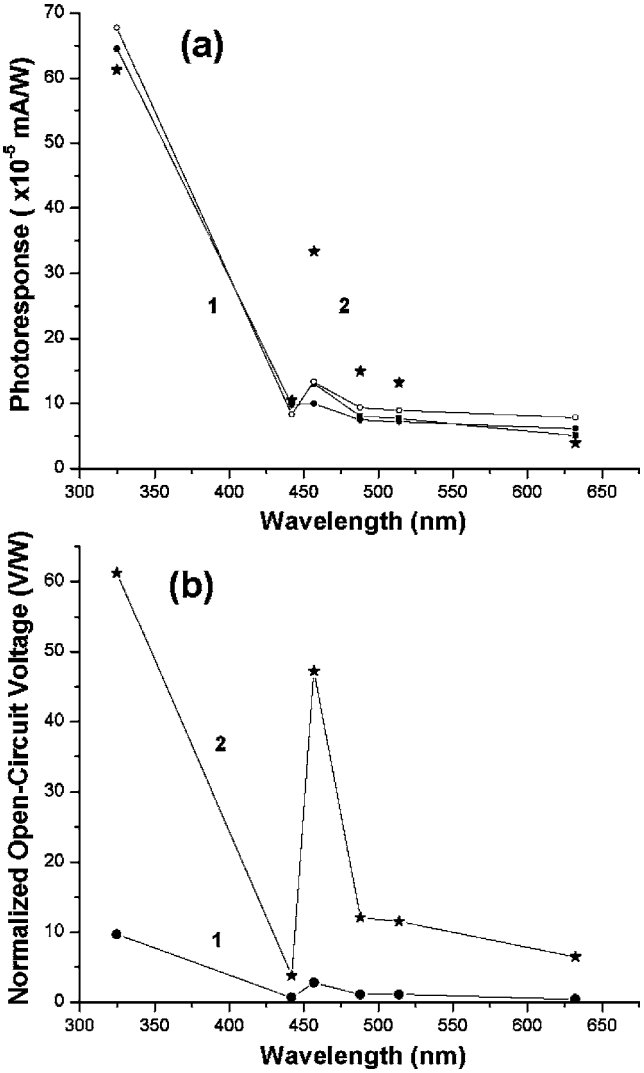

FIG. 3. Normalized photocurrent (a) and open-circuit voltage (b) for pristine *a*-Si–*c*-Si *p-n* junction (circles 1) and for nanocomposite device (stars 2) at various wavelengths.

have comparable photoresponses. This indicates to strong light absorption in the NC layer.

The NC device exhibits the strongest photoresponse at wavelengths 457, 488, and 514 nm, while at longer wavelength of 632 nm and at shorter wavelengths of 442 and 325 nm the photoresponse is very close to that of pristine silicon device. Amorphous silicon and PbSe films exhibit no peaks in absorption spectra at the wavelengths of 457, 488, and 514 nm. Therefore, the observed effect cannot be attributed only to increasing the material absorption at shorter wavelengths. At the effective bandgap of PbSe nanocrystals $E_g^*=0.8$ eV (corresponding to the first absorption peak of NCs at 1526 nm) the points of high photoresponse 457, 488, and 514 nm correspond to the excitation light with energy $3.3E_g^*$, $3.1E_g^*$, and $3.0E_g^*$, accordingly. It is just the region of about $3E_g^*$ where one should expect to observe the carrier multiplication effect, which has been demonstrated earlier in the time-resolved spectroscopy of biexcitons in NCs.[1–5] The points at 442 and 325 nm corresponding to the energies of $3.5E_g^*$ and $4.7E_g^*$ do not exhibit increasing the photocurrent. Probably, this can be explained by much faster Auger recombination of high-energy biexciton states in NCs.

The dependence of open-circuit voltage on wavelength shown in Fig. 3(b) is similar to that obtained for short circuit photocurrent. The voltage also exhibits a peak at wavelength 457 nm corresponding to the energy $3.3E_g^*$. Generally, the open-circuit voltage in the devices containing NCs is by one order of magnitude higher than that in pristine silicon *p-n* junction. Because the model NC device demonstrated both the increased photocurrent and increased open-circuit voltage, the NC photovoltaic materials can exhibit enhanced energy conversion efficiency.

The development of high-efficiency thin film amorphous silicon solar cells taking advantage of the demonstrated properties of the nanocrystal photovoltaic material requires fabrication of nanocrystal films exhibiting sufficiently high charge mobility. High charge mobility is needed for efficient transport of photogenerated electrons and holes through the intrinsic layer, which must have sufficiently large thickness in order to completely absorb solar light. During last several years the technologies for fabrication of quite thick (up to several microns) nanocrystal "solids" have been developed [10–12].

One of the main parameters determining losses in solar cells is the mobility-lifetime product, $\kappa=\mu\tau$, where μ is charge mobility and τ is characteristic lifetime of charge carriers. In a-Si material $\kappa\sim 10^{-8}\mathrm{cm}^2/V$ for holes and $\sim 10^{-7}$ cm^2/V for electrons. Although the charge mobility in NC solid films $\mu\sim 0.1\ \mathrm{cm}^2/V\,s^{-1}$ is of the order of hole mobility and ten times lower than electron mobility in a-Si, one can expect lower losses in NC films due to very long recombination lifetimes of charge carriers in PbSe nanocrystals (typical experimental value is ~1 microsecond independent of size). The mobility-lifetime product in PbSe NC films is expected to be of the order of 10^{-7} cm^2/V for both electrons and holes. Therefore, one can fabricate the nanocrystal a-Si based solar cells with the efficiency much higher than that achievable in currently manufactured conventional a-Si solar cells (~6–7.5 %) even if contribution of the carrier multiplication effect is small.

In conclusion, we fabricated nanocomposite *p-i-n* junctions based on hydrogenated amorphous silicon material, in which colloidal semiconductor NCs made of lead selenide (PbSe) form the intrinsic layer sandwiched between bulk *p*-type crystalline silicon (*c*-Si) and *n*-type hydrogenated amorphous silicon (*a*-Si:H) layer. Total thickness of the nanocrystal intrinsic layer in the samples was three to four NC diameters. Survival of the NCs after deposition of amorphous silicon has been demonstrated by observing photoluminescence and measuring absorption spectrum of NCs covered by an amorphous silicon layer. We also fabricated pristine *p*(*c*-Si)-*n*(*a*-Si) junctions without NCs for comparison of their properties with nanocomposite photovoltaic devices. Both pristine and nanocomposite devices have been fabricated using the same PECVD process for deposition of *a*-Si.

The current-voltage characteristics of pristine *p-n* junctions without nanocrystals demonstrate a behavior typical for *p-n* junctions, while current-voltage characteristics of nanocomposite *p-n* junctions demonstrate the presence of a nanocrystal intrinsic layer with quite low conductivity.

We also demonstrated the photocurrent in a NC intrinsic layer sandwiched between *n*- and *p*-type layers, i.e., the photovoltaic effect in NCs in the presence of a strong built-in electric field of the junction, which ejects photogenerated charges from the NCs. Both the short circuit photocurrent and open-circuit voltage for PbSe nanocomposite devices have been measured at six different wavelengths of light in the range of 325–632 nm.

At certain wavelengths exceeding three effective bandgap energies ($3E_g^*$) in NCs both the photocurrent and open-circuit voltage in the nanocomposite devices exhibited strong peaks. That peaks can be due to possible contribution of the carrier multiplication effect. More detailed study of this phenomenon is in progress. Because our model NC device demonstrated both the increased photocurrent and increased open-circuit voltage, the NC photovoltaic materials can exhibit enhanced energy conversion efficiency.

Some of the obtained results were independently confirmed in recent publication.[13] The authors demonstrated the CM effect in photocurrent through PbSe NC film of thickness 85 nm placed between two electrodes under applied bias voltage of 1 V. Internal photon conversion efficiency increased from 100% to 210% when photon energy increased from $2.8E_g^*$ to $4.4E_g^*$.

The research was funded by NSF SBIR Grant No. 0711509. The authors thank EPV Solar, Inc. for deposition of amorphous silicon films.

[1] R. D. Shaller and V. I. Klimov, Phys. Rev. Lett. **92**, 186601 (2004).
[2] R. Ellingson, M. C. Beard, J. C. Johnson, P. Yu, O. I. Micic, A. J. Nozik, A. Shabaev, and Al. L. Efros, Nano Lett. **5**, 865 (2005).
[3] R. D. Shaller, V. M. Agranovich, and V. I. Klimov, Nat. Phys. **1**, 180 (2005).
[4] A. Shabaev, Al. L. Efros, and A. J. Nozik, Nano Lett. **6**, 2856 (2006).
[5] R. Shaller, M. Sykora, J. M. Pietryga, and V. I. Klimov, Nano Lett. **6**, 424 (2006).
[6] A. J. Nozik, Advanced Concepts for Photovoltaic Cells, NCPV and Solar Program Review Meeting, 2003 (unpublished), NREL/CD-520-33586, p. 422.
[7] A. H. Mueller, M. A. Petruska, M. Achermann, D. J. Werder, E. A. Akhadov, D. D. Koleske, M. A. Hoffbauer, and V. I. Klimov, Nano Lett. **5**, 1039 (2005).
[8] R. A. Street, *Hydrogenated Amorphous Silicon* (Cambridge University Press, Cambridge 1991).
[9] S. G. Krivoshlykov and V. I. Rupasov, U.S. Patent Application No. 11/439,626 (24 May 2006).
[10] D. Yu, C. Wang, and P. Guyot-Sionnest, Science **300**, 1277 (2003).
[11] D. Talapin and C. Murray, Science **310**, 86 (2005).
[12] G. Konstantatos, I. Howard, A. Fisher, S. Hoogland, J. Clifford, E. Klem, L. Levina, and E. H. Sargent, Nature (London) **442**, 180 (2006).
[13] S. J. Kim, W. J. Kim, Y. Sahoo, A. N. Cartwright, and P. N. Prasad, Appl. Phys. Lett. **92**, 031107 (2008).